Catalysis Today 164 (2011) 457–460

Contents lists available at ScienceDirect

Catalysis Today

journal homepage: www.elsevier.com/locate/cattod

The effect of calcination temperature on the performance of Ni/MgO–Al_2O_3 catalysts for decarboxylation of oleic acid

Hyun-Seog Roh[a,*], Ic-Hwan Eum[a], Dae-Woon Jeong[a], Bo Eun Yi[b], Jeong-Geol Na[b], Chang Hyun Ko[b,**]

[a] *Department of Environmental Engineering, Yonsei University, 234 Maeji, Heungeop, Wonju, Gangwon 220-710, South Korea*
[b] *Greenhouse Gas Research Center, Korea Institute of Energy Research (KIER), 102 Gajeong-ro, Yuseong, Daejeon 305-343, South Korea*

ARTICLE INFO

Article history:
Available online 11 November 2010

Keywords:
Decarboxylation
Ni/MgO–Al_2O_3
Redox property

ABSTRACT

Ni catalysts supported on MgO–Al_2O_3 (MgO = 70 wt.%) were prepared at various calcination temperatures for decarboxylation of oleic acid. According to TPR patterns of Ni/MgO–Al_2O_3 catalysts, the reduction degree increases with decreasing the calcination temperature from 500 to 300 °C. Ni/MgO–Al_2O_3 catalyst calcined at 300 °C exhibited the highest oleic acid conversion as well as high selectivity to C_{17} compounds at the reaction temperature of 300 °C. This is due to free NiO species, which have relatively weak interaction with the support.

1. Introduction

The first generation of bio-diesel, fatty acid methyl ester (FAME), was produced via trans-esterification of lipids with methanol [1]. However, FAME bio-diesel has some disadvantages such as follows. FAME has high cloud point and pour point which can lead to clogging of fuel filters and supply lines at low temperatures [2]. Besides, the oxygenated compounds in FAME result in thermal instability, corrosiveness and low heating value [3]. Therefore, the elimination of the oxygenated compounds in FAME improves its stability and enhances its utilization potential. As a consequence, hydrodeoxygenation (HDO) process has been developed to remove the oxygenated compounds in lipids [4,5]. However, HDO process consumes excess hydrogen [6]. As an alternative, decarboxylation of lipids can be considered. Unlike HDO, decarboxylation does not require hydrogen and does not produce water, which causes catalyst deactivation [6].

Several active metals, such as Pd, Ni, Ru, Ir, Os, Rh supported on silica, alumina and activated carbon catalysts have been studied in the deoxygenation reaction [7]. The most efficient deoxygenation catalysts are precious metals such as Pt and Pd [7]. Since the precious metals are rare and expensive, some transition metal oxide and metal catalysts have been studied from economical point of view. Recently, Na et al. [6] reported that hydrotalcites (MgO–Al_2O_3) showed the activity of decarboxylation. However, the selectivity to heptadecene, a product by direct decarboxylation of oleic acid, was very low, implying that cracking and decarboxylation occurred simultaneously during the reaction by hydrotalcites. Takemura et al. [8] found that alumina-supported Ni catalysts were active for liquid-phase benzoic acid decarboxylation at 390 °C under H_2 or N_2 pressure in a batch autoclave. Moreover in a patent it has been described that straight chain olefins were produced from saturated fatty acids and fatty acid esters over Ni-based catalyst promoted with either tin, germanium or lead [9].

In this study, Ni catalysts supported on MgO–Al_2O_3 (MgO = 70 wt.%) calcined at various temperatures were prepared, characterized and applied to decarboxylation of oleic acid (cis-9-octadecenoic acid: $C_{17}H_{33}COOH$). The catalyst properties have been characterized by BET, XRD, TEM, TPR and related to the activity results in decarboxylation.

2. Experimental

2.1. Catalyst preparation

MgO–Al_2O_3 (MgO = 70 wt.%, SASOL) was employed as a support in this study. The support was pre-calcined at 500 °C for 6 h. $Ni(NO_3)_2 \cdot 6H_2O$ (97%, JUNSEI) was used as a precursor of Ni. Supported Ni catalysts were prepared by an incipient wetness impregnation method. The loading amount of Ni was fixed at 20 wt.%. The prepared catalysts were calcined at each temperature for 6 h. The prepared catalysts were reduced in a 10 vol.% H_2/Ar stream at 700 °C for 2 h and cooled down to room temperature in N_2.

2.2. Characterization

The BET surface area was measured by nitrogen adsorption at −196 °C using an ASAP 2010 (Micromeritics). The quantitative

---

* Corresponding author: Tel.: +82 33 760 2834; fax: +82 33 760 2571.
** Corresponding author: Tel: +82 42 860 3132; fax: +82 42 860 3134.
E-mail addresses: hsroh@yonsei.ac.kr (H.-S. Roh), chko@kier.re.kr (C.H. Ko).

0920-5861/$ – see front matter © 2010 Elsevier B.V. All rights reserved.
doi:10.1016/j.cattod.2010.10.048

Table 1
Characteristics of 20 wt.% Ni/MgO–Al_2O_3 (MgO = 70 wt.%) catalysts calcined at various temperatures.

Cal. temp. (°C)	SA_{BET} (m^2/g)		V_{pore} (cm^3/g)		Crystallite size (nm)	
	Fresh	Reduced	Fresh	Reduced	NiO/MgO	Ni^0
300	11	114	0.06	0.26	8.3	N.A.[a]
400	51	96	0.20	0.28	8.3	7.4
500	89	89	0.28	0.28	8.3	7.7

[a] Not available due to very weak XRD peak.

analysis of weight loss of the sample was performed with a thermogravimetric analyzer (TGA, Netzsch TG209F3). The XRD patterns were recorded using a Rigaku D/MAX-IIIC diffractometer (Ni filtered Cu-K radiation, 40 kV, 50 mA), and the crystallite size was estimated by using Scherrer equation [10]. Transmission electron microscopy (TEM) images of reduced catalysts were obtained in Tecnai F30S-Twin (FEI) microscope with 300 kV operating voltage. All samples were suspended in ethanol by ultrasonication. The suspension was deposited on a copper grid with hollow carbon film for TEM measurements. Temperature programmed reduction (TPR) was carried out in an Autochem 2910 (Micromeritics) using 10 vol.% H_2/Ar with a heating rate of 10 °C/min. The reduction degree was estimated by integrating the peak area of the reduction curve (from 100 to 950 °C) relative to the reference curve of NiO.

2.3. *Catalytic reaction*

The decarboxylation reactions were carried out in an autoclave reactor (100 mL) operating in a batch mode. The autoclave reactor was designed for operation up to 100 bar and 450 °C. A multi-blade impeller was equipped to mix liquid reactant and solid catalyst. The temperature was measured with a K-type thermocouple. In a typical batch experiment, 55.0 g of oleic acid and 1.375 g of catalyst (reactant/catalyst = 40/1 wt./wt.) were placed in the reactor. After oleic acid and catalyst were loaded in the reactor, the reactor was flushed with nitrogen to remove the remaining oxygen. Then, the reactor was heated to 300, 350, and 400 °C and the reaction temperature was maintained at each temperature for 3 h. The stirring speed was fixed at 800 rpm during the reaction. The reactor was subsequently cooled down to room temperature. The liquid products were collected after filtering solid phase catalysts.

The liquid products were analyzed by a gas chromatograph (HP 6890N) equipped with a flame ionization detector and a capillary column (HP-5, 30 m).

3. Results and discussion

3.1. *Catalyst characterization*

The characteristics of supported Ni catalysts are listed in Table 1. In the case of fresh catalysts, the BET surface area and pore volume dramatically increases with an increase of the calcination temperature from 300 to 500 °C. On the contrary, the BET surface area of reduced catalysts gradually decreases with increasing the calcination temperature from 300 to 500 °C. This indicates that the pore of the fresh catalyst calcined at 300 °C was filled with NiO and residual salt after calcination at 300 °C. According to thermogravimetric analysis (TGA) results, residual salt could be removed in the temperature range between 300 and 360 °C. After the reduction process, residual salt was eliminated and NiO species were reduced into Ni, resulting in an increase of BET surface area and pore volume. The degree of pore-filling of the catalyst strongly depends on the calcination temperature.

XRD patterns of fresh and reduced catalysts are shown in Fig. 1. All the fresh catalysts show characteristic peaks of MgO or NiO [11].

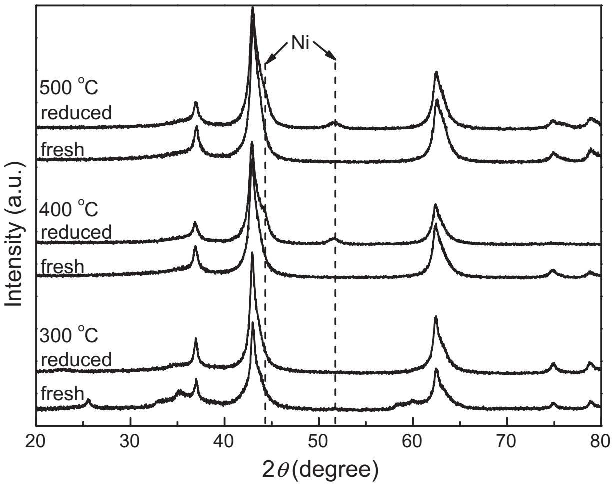

Fig. 1. XRD patterns of 20 wt.% Ni/MgO–Al_2O_3 (MgO = 70 wt.%) catalysts calcined at various temperatures.

It is difficult to distinguish MgO peaks from NiO peaks because the peaks overlap each other [12]. The crystallite size of MgO or NiO is calculated to be about 8.3 nm without regard to the calcination temperature of catalyst. As a consequence, the crystallite size of 8.3 nm can be assigned to that of MgO because the precalcination temperature of support was fixed at 500 °C. Thus, the NiO crystallite size is assumed to be less than 8.3 nm. For reduced catalysts, metallic Ni peak can be seen at 51.8° over the catalysts calcined at 400 and 500 °C. In the case of the reduced catalyst, which was calcined at 300 °C, metallic Ni peak does not appear. This indicates that the crystallite size of Ni is too small to be measured by XRD.

Fig. 2 displays the effect of calcination temperature on the formation of Ni particles. For the sample calcined at 300 °C, Ni particles cannot be found. This indicates that Ni is finely dispersed on support. For the samples with 400 and 500 °C calcinations, Ni particles with ca. 8 nm diameter are dispersed on substrates. The particle sizes observed in TEM images are consistent with those calculated by using XRD patterns (Table 1).

Fig. 3 depicts TPR patterns of Ni/MgO–Al_2O_3 catalysts calcined at different temperatures. Table 2 summarizes the reduction degree of NiO. In general, the peak appearing at around 400 °C is attributed to the reduction of the relatively free NiO species, which have no interaction or weak interaction with support, while the peak appearing at about 600 °C is assigned to the reduction of complex NiO species,

Table 2
Reduction degree of 20 wt.% Ni/MgO–Al_2O_3 (MgO = 70 wt.%) catalysts calcined at various temperatures.

Cal. temp. (°C)	Reduction degree (%, free NiO)	Reduction degree (%, complex NiO)	Reduction degree (%, total)
300	56	42	98
400	22	46	68
500	7	49	56

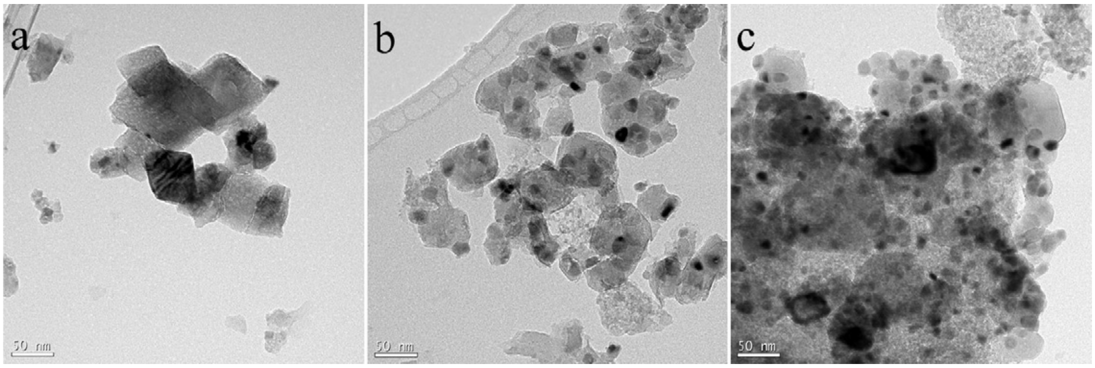

Fig. 2. TEM images of 20 wt.% Ni/MgO–Al_2O_3 (MgO = 70 wt.%) catalysts calcined at various temperatures: (a) 300 °C, (b) 400 °C, and (c) 500 °C (after calcinations, all samples were reduced at 700 °C).

which have intimate contact with support. The reduction peak appearing at around 800 °C can be assigned to the reduction of the NiO species, which are incorporated into the support lattice [13]. For the catalyst calcined at 300 °C, the first reduction peak of NiO appears at 360 °C, which can be assigned to free NiO species. The second peak appearing at around 800 °C is assigned to the reduction peak of incorporated NiO species. The higher the calcination temperature, the deeper NiO becomes incorporated into the support lattice. As a result, free NiO species decrease remarkably, while incorporated NiO species increase with an increase of the calcination temperature from 300 to 500 °C. In addition, total reduction degree decreases with increasing the calcination temperature from 300 to 500 °C.

3.2. Reaction results

Table 3 summarizes reaction results over Ni/MgO–Al_2O_3 catalysts. At the reaction temperature of 300 °C, Ni/MgO–Al_2O_3 catalysts exhibited 5–6 times higher oleic acid conversion than blank test without catalyst. This indicates that catalytic reaction occurred at this temperature. Furthermore, the oleic acid conversion of the catalyst calcined at 300 °C is about 5% higher than those of catalysts calcined at 400 and 500 °C. Therefore, it has been confirmed that free Ni species, reduced from free NiO species, have beneficial effect on decarboxylation of oleic acid. In the case of blank test, the selectivity to stearic acid (36.7%) is much higher than those of catalysts. Stearic acid is considered as a reaction intermediate for decarboxylation of oleic acid [14]. As a result, metallic Ni species are expected to be active sites to produce C_{17} compounds, which are desirable products in decarboxylation of oleic acid from stearic acid. The selectivities to C_{17} compounds are about 5% over catalysts irrespective of the calcination temperature (Fig. 4). At the reaction temperature of 350 °C, blank test without catalyst showed 61.8% oleic acid conversion. The support (MgO–Al_2O_3, MgO = 70%) showed similar reaction results to blank test without catalyst at this temperature. Ni/MgO–Al_2O_3 catalysts calcined at 400 and 500 °C showed 60.5 and 63.6% oleic acid conversion, respectively. The catalyst calcined at 300 °C exhibited the highest oleic acid conversion. It is most likely that both thermal reaction and catalytic reaction took place simultaneously at this reaction temperature. However, the selectivity to C_{17} compounds depends strongly on the catalyst (Fig. 4). The selectivities to C_{17} compounds of the catalysts calcined at 400 and 500 °C are twice higher than that of blank test. Moreover, the catalyst calcined at 300 °C shows 3 times higher selectivity to C_{17} compounds than the blank test. Thus, it is also confirmed that free Ni species have positive effect on production of C_{17} compounds. At the reaction temperature of 400 °C, oleic acid conversions are higher than 98%. This indicates that thermal reaction is favorable at this reaction temperature due to pyrolysis of oleic acid [15]. However, the selectivity to C_{17} compounds depends on the catalyst. The selectivity to C_{17} compounds of the catalyst calcined at 300 °C is the highest.

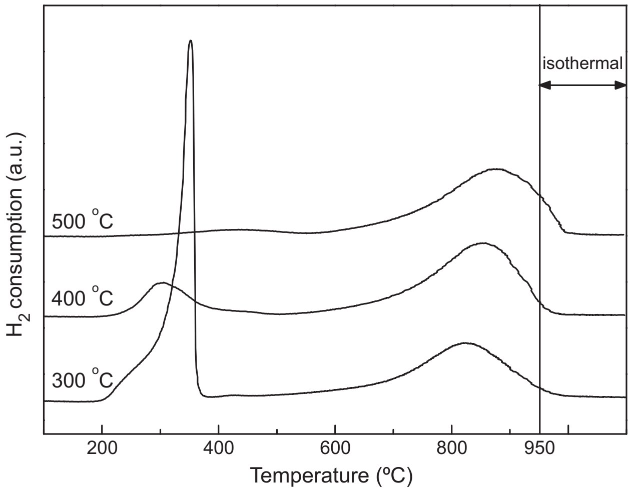

Fig. 3. TPR patterns of 20 wt.% Ni/MgO–Al_2O_3 (MgO = 70 wt.%) catalysts calcined at various temperatures.

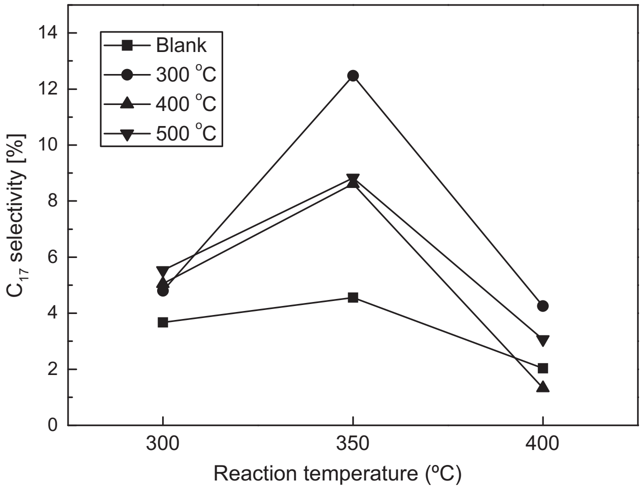

Fig. 4. Selectivity to C_{17} compounds (heptadecane and 8-heptadecene) over 20 wt.% Ni/MgO–Al_2O_3 (MgO = 70 wt.%) catalysts calcined at various temperatures.

Table 3
Reaction results of decarboxylation of oleic acid over 20 wt.% Ni/MgO–Al_2O_3 (MgO = 70 wt.%) catalysts calcined at various temperatures.

Cal. temp.	Rxn. temp.								
	300 °C (%)			350 °C (%)			400 °C (%)		
	$X_{O.A.}$	S_{C17}[b]	$S_{S.A.}$[c]	$X_{O.A.}$	S_{C17}[b]	$S_{S.A.}$[c]	$X_{O.A.}$	S_{C17}[b]	$S_{S.A.}$[c]
Blank[a]	5.2	3.7	36.7	61.8	4.6	5.2	99.5	2.0	1.4
300 °C	31.3	4.8	10.1	67.5	12.5	3.3	99.3	4.3	0.1
400 °C	27.5	5.0	10.6	60.5	8.6	3.9	99.5	1.3	0.0
500 °C	26.0	5.5	12.3	63.6	8.8	4.6	98.4	3.1	0.2

[a] Blank test without catalyst.
[b] Selectivity to 8-heptadecene or heptadecane.
[c] Selectivity to stearic acid.

In summary, catalytic decarboxylation is a major reaction pathway at the reaction temperature of 300 °C. At the reaction temperature of 350 °C, both catalytic reaction and thermal reaction are reaction pathways. It is most likely that 350 °C is an optimum reaction temperature because C_{17} selectivity is the highest at this temperature. At the reaction temperature of 400 °C, thermal reaction is dominant. Although the conversion of oleic acid is enhanced with an increase of the reaction temperature, C_{17} selectivity is decreased due to pyrolysis of oleic acid.

4. Conclusion

Catalytic decarboxylation of oleic acid is dominant at the reaction temperature of 300 °C. Both catalytic reaction and thermal reaction take place at the reaction temperature of 350 °C. Thermal reaction is favorable at the reaction temperature of 400 °C due to pyrolysis of oleic acid. The Ni/MgO–Al_2O_3 catalyst calcined at 300 °C exhibited the highest oleic acid conversion at the reaction temperature range from 300 to 350 °C. This catalyst also showed the highest selectivity to C_{17} compounds at 350 °C. This is mainly due to the presence of free Ni species, which have beneficial effect on decarboxylation of oleic acid.

References

[1] http://siteresources.worldbank.org/INTWDR2008/Resources/2795087-1191440805557/4249101-1191956789635/Brief_BiofuelPrmsRisk_web.pdf.
[2] S.M. Geyer, M.J. Jacobus, S.S. Lestz, Trans. ASAE 27 (1984) 375.
[3] J.P. Diebold, A review of the chemical and physical mechanisms of the storage stability of fast pyrolysis bio-oils, in: A.V. Bridgwater (Ed.), Fast Pyrolysis of Biomass: A Handbook, vol. 2, Cpl Press, UK, 2002, p. 243.
[4] G.W. Huber, P. O'Connor, A. Corma, Appl. Catal. A: Gen. 329 (2007) 120.
[5] A. Centeno, E. Laurent, B. Delmon, J. Catal. 154 (1995) 288.
[6] J.-G. Na, B.E. Yi, J.N. Kim, K.B. Yi, S.-Y. Park, J.-H. Park, J.-N. Kim, C.H. Ko, Catal. Today 156 (2010) 44.
[7] M. Snåre, I. Kubic-ková, P. Mäki-Arvela, K. Eränen, D.Y. Murzin, Ind. Eng. Chem. Res. 45 (2006) 5708.
[8] Y. Takemura, A. Nakamura, H. Taguchi, K. Ouchi, Ind. Eng. Chem. Prod. Res. Dev. 24 (1985) 213.
[9] R. Sterrn, G. Hillon, US Patent 4,554,397 (1985).
[10] H.S. Potdar, H.-S. Roh, K.-W. Jun, M. Ji, Z.-W. Liu, Catal. Lett. 84 (2002) 95.
[11] K.Y. Koo, H.-S. Roh, U.H. Jung, D.J. Seo, Y.-S. Seo, W.L. Yoon, Catal. Today 146 (2009) 166.
[12] K.Y. Koo, H.-S. Roh, Y.T. Seo, D.J. Seo, W.L. Yoon, S.B. Park, Appl. Catal. A: Gen. 340 (2008) 183.
[13] H.-S. Roh, H.S. Potdar, K.-W. Jun, J.-W. Kim, Y.-S. Oh, Appl. Catal. A: Gen. 276 (2004) 231.
[14] M. Snåre, I. Kubic-ková, P. Mäki-Arvela, D. Chichova, K. Eränen, D.Y. Murzin, Fuel 87 (2008) 933.
[15] K.D. Maher, K.M. Kirkwood, M.R. Gray, D.C. Bressler, Ind. Eng. Chem. Res. 47 (2008) 5328.